

Document downloaded from:

<http://hdl.handle.net/10251/115874>

This paper must be cited as:

Parra-Boronat, L.; Rocher-Morant, J.; Escrivá-Perales, J.; Lloret, J. (2018). Design and development of low cost smart turbidity sensor for water quality monitoring in fish farms. *Aquacultural Engineering*. 81:10-18. doi:10.1016/j.aquaeng.2018.01.004



The final publication is available at

<https://doi.org/10.1016/j.aquaeng.2018.01.004>

Copyright Elsevier

Additional Information

# Design and development of low cost smart turbidity sensor for water quality monitoring in fish farms

Lorena Parra, Javier Rocher, Julia Escrivá and Jaime Lloret

Instituto de Investigación para la Gestión Integrada de zonas Costeras. Universitat Politècnica de València, Spain

Email: [loparbo@doctor.upv.es](mailto:loparbo@doctor.upv.es), [jarocmo@alumni.upv.es](mailto:jarocmo@alumni.upv.es), [juespe@epsg.upv.es](mailto:juespe@epsg.upv.es), [\\_jlloret@dcom.upv.es](mailto:_jlloret@dcom.upv.es)

**Abstract**— Turbidity monitoring is necessary in many cases and several sensors have been developed for this purpose. However, in some cases to quantify the turbidity it is not enough and its characterization is necessary. In fish farms, the increase of sedimentary or phytoplanktonic turbidity requires different actions to prevent further damages. For this reason, a sensor able to differentiate between turbidity sources is necessary. In this paper, a turbidity sensor able to distinguish different types of turbidity is designed, developed and calibrated. The sensor is based on the Beer-Lambert law and it uses four LEDs as light sources with different wavelengths. The sensing elements are located at 180° of the light sources and consist of a photodiode and a photoresistor, sensitive to infrared and visible wavelengths respectively. For the calibration process different turbidity sources were employed, *Isochrysis galbana*, *Tetraselmis chuii* and sediment. The results show that it is possible to determine the turbidity using the infrared light and to characterize the origin of that turbidity with the red light. An algorithm was created in order to create a method to process the data from each sample to obtain the turbidity, the origin of this turbidity and the concentration of the turbidity source. With this algorithm, we can create a smart turbidity sensor for water quality monitoring. Our main application is focused on monitoring the water input in fish farm facilities; however, this smart sensor will be useful in many other areas.

**Index Terms**— turbidity sensor; phytoplankton; suspended sediment; water quality; fish farms

## I. INTRODUCTION

The increase in human population and the changes of land use increase the turbidity levels in water (Fabricius et al., 2016). The monitoring of turbidity, for different purposes, has become an important issue. Turbidity is caused by suspended particles in water; these substances may be organic or inorganic. The inorganic ones are mainly composed of sediments, while the organic ones are mainly algae, microorganism, etc... (MPCA, 2017 and APHA, AWWA, WEF, 2012). Turbidity measurements are necessary for water quality monitoring. It is measured in natural resources, because of the negative effects on ecosystems (Smith & Davis-Colley, 2001). Moreover, it is measured in drinking water (Beaudeau et al., 2014), or in irrigation water (PNUMA, 2017). The principal effects of turbidity in the ecosystems are (I) reduction of visibility, (II) reduction of light penetration and photosynthesis process or (III) clogging of gills and other adverse physical effects on fish and eggs (Bruton, 1985 and Wilber & Clarke 2001) among others. However, in some cases, the quantitative value of turbidity is not enough, because different types of turbidity may cause different effects. One example is in the fish farms, where the turbidity generated by sediments and the one generated by phytoplankton can require different actions to prevent further damages. For this reason, the characterization of turbidity is needed in the fish farms and in many other cases.

In fish farming, the increase of turbidity causes a reduction of fish performance. The effects of turbidity on fish growth and survival have been studied by different authors. Sutherland & Meyer (2007) maintained two fish species from 0 to 500 mg/l of sediment during 21 days. Their results showed that *Erimonax monachus* presented the highest SGR at 0 mg/l while *Cyprinella galactura* presented it from 0 to 50mg/l. Ardjoosediro & Ramnarine (2002) maintained red tilapia during 56 days at different turbidity values, from

0 to 500 mg/l of clay. Fish presented higher weight at the end of the experiments when the level of turbidity was lower. The maximum survival rates were reached from 0 to 50mg/l.

The possibility of monitoring the values of turbidity at the water input in the aquaculture facilities is useful in order to take different actions to prevent further damages in fish production. It can be especially valuable for inland facilities with open water circuit. In the facilities where larval and reproducers are kept those sensors are crucial to ensure the water quality in the production tanks. However, different types of turbidity cause different effects on fish. Suspended sediment may cause gill damage. *Cyprinella galactura* shows no gill damage from 0 to 50 mg/l of sediment, moderate damage at 100 mg/l and severe at 500 mg/l (Sutherland & Meyer, 2007). Au et al., (2004) founded a correlation on *Epinephelus coioides* between gill damage and suspended sediments. Hess et al., (2015) studied the changes in gills morphology on clownfish larvae exposed to suspended sediments. They conclude that fish exposed to 45 mg/l of sediments or more, had excessive mucous discharge and growth of protective cell layers. Moreover, in facilities with larvae culture, the technique of greenwater is widely used to increase the growth and survival of larvae (Faulk & Holt, 2005 and Palmer et al., 2007). This technique consists of adding algae in the water of the larvae tanks. However, this technique requires aeration to ensure the appropriate oxygen levels and to avoid the phytoplankton sedimentation. Recently, the use of clay has been studied as a substitute for phytoplankton in *Anoplopoma fimbria* (Lee, 2015a and Lee et al., 2017). However, the use of the greenwater technique requires the use of aeration to ensure that the oxygen concentrations do not decrease during dark periods. Different turbidity can cause different effects on fish and some specific actions must be taken. For this reason, it is necessary to have an automatic method to monitor the turbidity and to characterize it. Then, we can differentiate between two types of turbidity in fish farms, sedimentary turbidity, and phytoplanktonic turbidity. The worse possible conditions are related to the appearance of phytoplankton turbidity during dark periods (night or dark photoperiod in the tanks). In those conditions, the phytoplankton starts to consume the oxygen in the water and may require the activation of the aeration in order to prevent hypoxia conditions in the tanks. Moreover, some algae species may produce toxic products.

There are other areas where characterize the turbidity may be useful. The possibility to detect and track phytoplankton blooms is interesting in some ecosystems, Parra et al. (2015) proposed a similar system with hydrocarbons. The algae blooms formed by some species are considered as an abnormal situation in ecosystems that can cause eutrophication. Moreover, in some cases, those algae blooms can produce water pollution because of the production of some toxic compounds by the algae. Besides, in dark conditions, the algae blooms may consume high quantities of dissolved oxygen.

The most common method for measuring turbidity is the optical sensors. Optical sensor works by emitting a beam of light and detecting the amount of light that reaches the detector. Three techniques exist for optical sensing, according to the measuring angles. If the angle is 90° it is called nephelometric, if the angle is 180° it is called absorbimeters and if the angle is found between 90° to 180° it is called backscattering (Bin Omar & Bin MatJafri, 2009). Different techniques are applied to measure different turbidity levels (Lambrou et al., 2009). Takaaki et al., (2012) used 5 stations with optical sensors to monitor sediment transported in rivers. Schoellhamer & Wrightl (2003) used optical turbidity sensors for continuous measurement of suspended solids discharged in rivers. Stubblefield et al., (2007) used nephelometric turbidimetry for determining suspended solids in a lake. The Secchi disk, a traditional method, consists of the introduction of a disk into the water, the distance in which we stop observing the disk is inversely proportional to the turbidity (Lee, 2015b). However, this methodology is not suitable for continuous monitoring. There are other methods such as acoustic sensors or the use of satellite images. Chanson et al., (2008) and Ward et al., (2013) used acoustic methods to measure the turbidity in rivers. Güttler et al., (2013) and Zheng et al., (2016) used remote sensing in rivers and lakes. The commercial turbidimeters that are currently in the market have two problems. The first one is the high price of the sensor, which may become prohibitive for many applications. The second one is that commercial sensors do not differentiate the type of turbidity (sedimentary or phytoplanktonic). Those are the current gaps in the commercial devices that are avoiding the use of turbidity sensors for monitoring in many applications.

In this paper, a low cost smart turbidimeter is designed and developed. Our smart turbidity sensor will be capable of differentiating phytoplanktonic turbidity from sedimentary turbidity. This new turbidimeter is based on optical methods. Different light-emitting diodes (LEDs) with different wavelength (i) infrared (IR), (ii) green, (iii) yellow and (iv) red are used as a light source. Two light detectors are used, a light dependent resistance (LDR) to detect visible light (180 °) and photodiodes for detecting infrared light. These light-emitting diodes (LEDs) are powered by a voltage of 4.5 V. The proposed sensor offers two improvements compared to existing commercial sensors: (i) the lower cost of the sensors and (ii) its capability to differentiate sedimentary turbidity from phytoplanktonic turbidity. This sensor will help us to control sensitive areas, monitor of fish farms. Moreover, it can be used in other activities or environments where a bloom of algae can be produced or the turbidity have to be controlled.

## II. MATERIAL AND METHODS

In this section, the material and methods are presented. First, the background about the light absorption and the turbidity is detailed. Then, the design and development and price of the turbidity sensor and the origin of turbidity samples are described.

### A. Background

In this section, the background of optical sensors are shown. Turbidity is defined as the loss of clarity in water, light may be absorbed, reflected or dispersed (Bin Omar & Bin MatJafri, 2009). Moreover, this parameter is related to the Beer-Lambert law Eq. (1) (Postolache et al., 2002). The Beer-Lambert law quantifies the transmitted light ( $I_t$ ), as a function of the light intensity of a source ( $I_o$ ), the absorption coefficient per unit length ( $a$ ), the turbidity ( $t$ ), and the length of the light pass ( $l$ ). From one side, absorption coefficient, and turbidity are related to the turbidity of the water. By the other side, the intensity of a source and length of the light pass are related to the measurement instrument. The value of ( $I_t$ ), can be expressed as a function of the scatter angle ( $\theta$ ), the particle size ( $r$ ), the wavelength( $\lambda$ ), and the optical properties of the particle and the medium such as the refractive index ( $n$ ) Eq. (2), (Postolache et al., 2002).

$$I_t = I_o \times e^{-(a*t)l} \quad (1)$$

$$I_t = I_o(\theta, \lambda, r, n) \quad (2)$$

### B. Design and development of the turbidity sensor

In this subsection the design and the development of our turbidity sensors are detailed. For its design, several conditions must be met. These include low cost, low battery consumption, low maintenance and easiness to clean. As we concluded in the previous section, the most suitable option is the use of light beam for turbidity detection. In the majority of papers, authors use IR light source and IR light detectors. Nevertheless, as the developed turbidity sensor must be able to distinguish between different turbidity sources, more than one light source will be included. One IR and three colour light sources, green, yellow and red. The 5mm IR LED employed is the TSHG6200 (Vishay, 2017a). It has a peak wavelength of 850nm. The 5mm colour LEDs sources have a peak wavelength of 612-625nm ( the red one), 581-594nm ( the yellow one) and 562-575nm (the green one). They are the TLLR4400 (Vishay, 2017b).The light receptors used in the sensor are the IR photodiode and the Light Dependent Resistor (LDR) is sensible to a visible light range, the used one is the NSL 19M51 (LDR, 2017). The IR photodiode employed presents high speed and high radiant sensitivity. Its sensitivity range goes from 790 to 1050nm and the peak is at 950nm. The photodiode is manufactured by Vishay, the code is BPW83 (Vishay, 2017c). The price of those materials is detailed in Table I. This price only includes the materials needed for the physical creation of the sensor, the sensing part: LEDs, light detectors, and resistors. The price of the Flyport or other nodes as Arduino or Waspote that can be used for the same purpose (Parra et al., 2017 and Sendra et al., 2013b) are not included. However, the price of simple Arduino modules is less than 10€. Besides, the possible resistors needed for the conditioning circuit, to regulate the input signal to the node, must be added.

Table 1. Price of the electronic components for the low cost smart turbidimeter

Component	Code	Producer	Price (€)
IR LED	TSHG6200	Vishay	1.15
Color LED (x3)	TLLR4400	Vishay	0.36 (x3)
IR detector	BPW83	Vishay	0.88
Color detector	NSL 19M51	Advanced Photonix	0.80
Resistor (x2)	PPC470BCT-ND	Vishay	0.27 (x2)
Total			4.45

The prototype can be seen in Figure 1. The light detectors are placed at 180° of the light sources. The distance between the light source and light detector are 6.5cm. A pipe made of non-porous crystal with a thickness of 2mm and a diameter of 2.7cm is employed to allow the water pass. The system of light sources and light receptors are placed inside a plastic box in complete darkness. Tubes of PVC are used to conduct the light of the LEDs to the crystal pipe. The same system is used with the receptors. Thus, we ensure that the light received at the light detector is the light of the LED that is not absorbed by the sample. The tubes have a length of 2cm from the light source to the crystal pipe and 1.4cm from the pipe to the receptor. The LEDs are powered using a Flyport module, which offers a constant output voltage of 4.6V. A resistor of 470 Ohms 5% is used between the Flyport and the LEDs to avoid possible damages. The value of resistor of the LDR and the photodiode are measured with a digital multimeter. The LEDs are powered sequentially: IR, red, yellow and green.

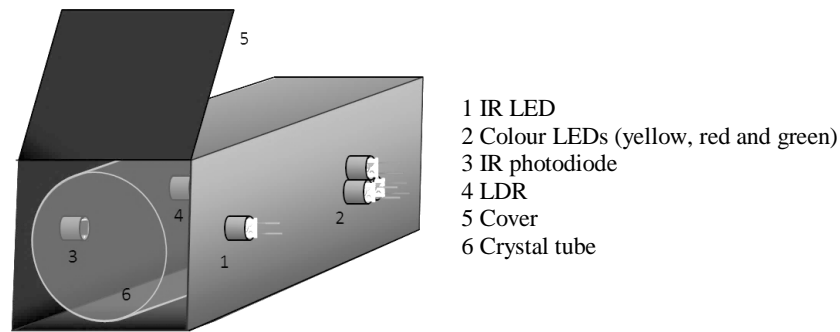


Figure 1. Representation of the prototype

### C. Turbidity samples

In this subsection, the different samples used in the process of sensor calibration are described. Three different types of samples are employed in the tests; the samples are composed of water and a turbidity source. The water is composed of distilled water and NaCl is added to reach a salinity of 36mg/l. It is necessary to work with that salinity because our objective is to use the sensor for marine water. The turbidity sources employed are *Isochrysis galbana* as brown algae, *Tetraselmis chuii* as green algae and brown silt as sediment. The original samples composed of algae have a concentration of 13.327.658cell/ml *Isochrysis galbana* and 1.818.056cell/ml *Tetraselmis chuii*. The algae used for calibration were obtained from pure cultures of *Isochrysis galbana* and *Tetraselmis chuii*. Both species were grown in filtered and sterilized seawater, enriched with F/2 medium adapted from Keller et al., (1987). These cultures were maintained at 25±1°C and continuous aeration, under a 12:12h light:dark photoperiod. Different dilutions of those samples are prepared to calibrate the sensor. The sediment used was obtained from a riverbed it is composed mainly of silt and a small percentage of sand. The soil was dried up using an oven at 40°C during 24h. The coarse materials were removed after the sample was dried up. On the other side, the samples composed of sediment are prepared, each one separately by weighing different amounts of silt and adding 70ml of distilled water.

The salty water was only used for the samples with phytoplankton, to avoid the lysis of the cells. However, to ensure that the different salinities do not affect to our device a preliminar test was carried out with

distilled water and salty water with no turbidity sources. The results show that the diluted salts do not affect to the light absorption.

### III. RESULTS AND DISCUSSION

In this section, the results are shown and the discussion is done. First, the results of light absorption of different turbidity sources are presented. Following, the mathematical model to distinguish different turbidity samples are shown. Then, the intelligent algorithm is explained and the verification process is carried out. Finally, a comparison between our developed system and the current options is done.

#### A. Different turbidity sources

In this section, we are going to analyze the results obtained from each one of the turbidity sources. First, the results of the samples that contain *Isochrysis galbana* as a turbidity source are shown. The resistance of the LDR and the IR photodiode are presented in Figure 2. The resistance of the IR photodiode increases as the concentration of the turbidity source decreases in a constant and linear pattern. By the other side, the relation between the resistance of the LDR and the turbidity is positive and exponential. It is possible to detect that each light presents different threshold values, from which is not possible to detect changes in turbidity. By the other side, there is a point where resistances maintain constant when the turbidity decreases. These threshold values are reached with the green light at 30% of dilution (3,998,297 cell/mL) with a constant resistance of 46.76M $\Omega$  and by the yellow light are 20% (2,665,532 cells/mL) of dilution with a constant resistance of 1.81M $\Omega$ . Those are the limits of detection (LOD) for the brown seaweed. The red light and IR light do not present LOD with the employed samples.

Following, the results with the samples with *Tetraselmis chuii* as a turbidity source are detailed. The results can be seen in Figure 3. The resistance of IR photodiode and the LDR are similar to the test with the *Isochrysis galbana*. The LOD is reached with the green light at 5% of dilution (90,903 cells/ml), with a resistance value of 46.7 M $\Omega$ . Moreover, the yellow light presents the LOD at 5% of dilution with a resistance value of 1.81M $\Omega$ . The maximum resistance is 92.63 M $\Omega$  in green, 24.27 M $\Omega$  in red, 7.77 M $\Omega$  in yellow and 8.66 M $\Omega$  in IR.

Finally, the results with the sediment as a turbidity source are shown in Figure 4. As in the other cases, the relation between turbidity and resistance of LDR is exponential. However, in this case, the relation between turbidity and IR photodiode is a negative exponential relation. The LOD was not detected for any light source. Nevertheless, for the green light, an upper limit value has been found. With more than 373 mg/l of sediment and a value of resistance of 200 M $\Omega$ , it is not possible to detect changes in green light absorption. The value of 200 M $\Omega$  corresponds to the highest value or the LDR (resistance in darkness). The sample with the highest concentration gives as a result 200 M $\Omega$  with all the lights.

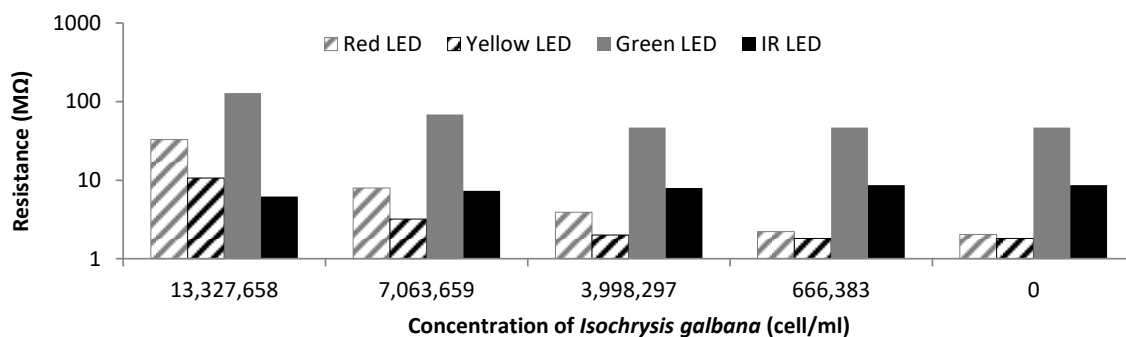


Figure 2. Resistance of LDR and photodiode with samples of *Isochrysis galbana*

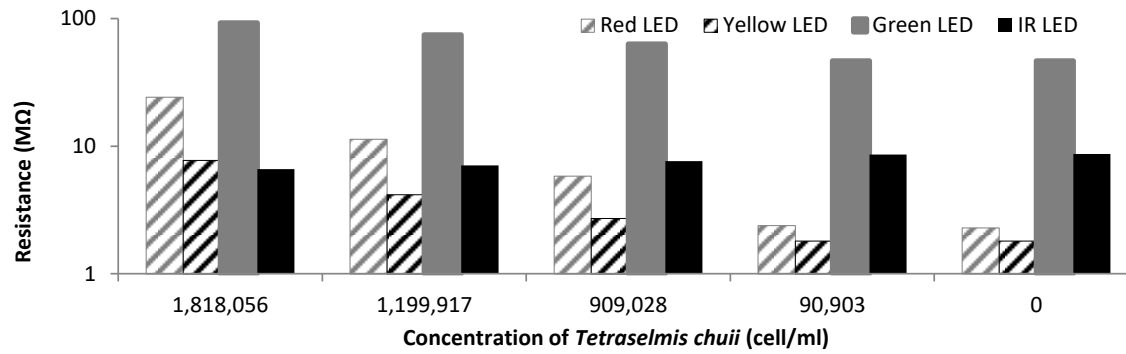


Figure 3. Resistance of LDR and photodiode with samples of *Tetraselmis chuii*

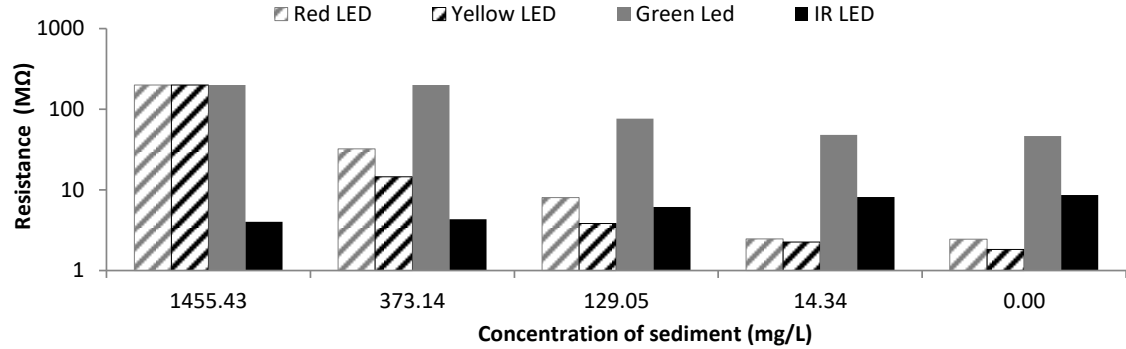


Figure 4. Resistance of LDR and photodiode with samples of Sediment

Our turbidity sensor is capable to distinguish between different concentrations of sediment, from 0 mg/l to 378mg/l. It is possible to distinguish higher values up to 1455 mg/l but only with IR light. For the turbidity generated with seaweed, we can distinguish between different concentrations form 0cells/mL to 13.327.658 cells/mL in *Isochrysis galbana* and from 0cells/mL to 1.818.056 cells/mL in *Tetraselmis chuii*. It is possible to distinguish higher concentration, but they are not tested. With the employed samples no LOD has been found. It is necessary to develop more analysis to found the LOD of the IR light absorption in our system.

#### B. Distinguish between turbidity sources

In this subsection the possibility to distinguish between different turbidity sources is shown. To compare between turbidity sources (sediments, green and brown algae) it is necessary to use turbidity units as Nephelometric Turbidity Unit (NTU). First of all, it is necessary to have a relation between the concentration in mg/l or in cells/mL and the NTU. For this purpose, the Eq. (3) shown in Sendra et al., (2013a), is used to relate the mg/l of sediment with NTU. Using this equation it is possible to relate the values of resistance of IR photodiode ( $R$ ) with the turbidity values Eq. (4). To obtain the Eq. (4) we relate the values of the IR photodiode obtained during the experiment with the values of turbidity in NTU obtained from applying the Eq. (3) to the samples of sediment. To relate those values the mathematical software (Eureqa, 2017) is used. The Eq. (5) and Eq. (6) are obtained by relating the values of turbidity in NTU calculated with Eq. (4) and the values of concentration for each one of the phytoplankton species.

$$\text{Sediment (NTU)} = 1.873 + 0.518 \times \text{Sediment (mg/L)} \quad (3)$$

$$\text{Turbidity (NTU)} = \frac{5209}{1.23 + R_{ir}(\text{M}\Omega)^2} - 66.72 \quad (4)$$

$$\text{Isochrysis galbana (NTU)} = 0.000005 \times \text{Isochrysis galbana} \left(\frac{\text{cell}}{\text{ml}}\right) - 2.6871 \quad (5)$$

$$\text{Tetraselmis chuii (NTU)} = 0.00005 \times \text{Tetraselmis chuii} \left(\frac{\text{cell}}{\text{ml}}\right) - 1.3232 \quad (6)$$

Now, it is possible to compare the resistance values of LDR with different lights for different turbidity sources. Thus, we can find a mechanism to differentiate different turbidity sources. For this purpose the software Statgraphics Centurion (STATGRAPHICS, 2017) is employed. Simple regression is used to obtain an equation that relates the resistance of LDR and the NTU for differences in the turbidity sources. The type of regression model used is an exponential model with a constant and it is based on the minimum squares adjustment. The confidence interval of each model is represented in the following figures. Our objective is, for each one of the lights (green, yellow and red), to present the obtained regression model with their confidence intervals for each turbidity source. Besides, it is necessary to evaluate if it is possible to distinguish different turbidity sources according to the confidence intervals.

First, the results obtained with green light are presented in Figure 5. It is possible to see the different regression models with their confidence intervals for each one of the turbidity sources. The different dashes represent different turbidity sources, short dashes for *Tetraselmis chuii*, long dashes for *Isochrysis galbana*, and no dashes for sediment. In squares are presented the gathered data in the previous subsection. The different lines represent the mathematical model in bold and the confidence intervals. The models represented in Figure 5 correspond to Eq. (7), Eq. (8) and Eq. (9).  $R_{green}$  (MΩ) represents the value of resistance in MΩ of the LDR exposed to green light. The value of  $R_{green}$  (MΩ) for the same turbidity value is different according to the turbidity source. For this reason, we distinguish between  $R_{green}$  if  $IG$  which represents the value of resistance of the LDR with *I. galbana*,  $R_{green}$  if  $TC$  or  $R_{green}$  if  $S$  depending if the turbidity source is *Tetraselmis chuii* or sediment. The turbidity of *Isochrysis galbana* (TIG), *Tetraselmis chuii* (TTC) or sediment (TS) represents the values of turbidity in each test. The correlation coefficients of those mathematical models are 0.985315, 0.983612 and 0.994686 respectively. The means absolute errors are 0.0489981, 0.0326879 and 0.0382279 NTU. According to the confidence intervals, see the Figure 5, it is possible to affirm that for values of turbidity higher than 47 NTU, our prototype is able to distinguish between phytoplanktonic turbidity and sedimentary turbidity. However, with green light, our device is not able to distinguish between *Tetraselmis chuii* and *Isochrysis galbana*, according to the confidence intervals.

$$R_{green\ if\ IG}(M\Omega) = e^{(3.75453 + 0.0171214 \times TIG\ (NTU))} \quad (7)$$

$$R_{green\ if\ TC}(M\Omega) = e^{(3.85743 + 0.0134761 \times TTC\ (NTU))} \quad (8)$$

$$R_{green\ if\ S}(M\Omega) = e^{(3.81816 + 0.00760528 \times TS\ (NTU))} \quad (9)$$

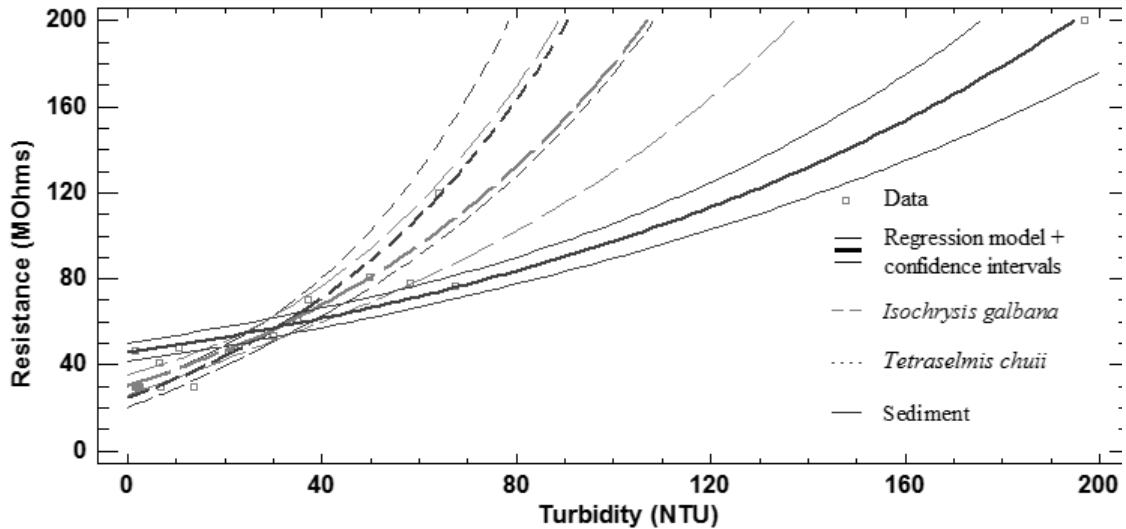


Figure 5. Regression models with confidence intervals for different turbidity sources with a green light.

Now, the results obtained with yellow light are presented. In the Figure 6, it is possible to see the three different regression models with their confidence intervals for each one of the turbidity sources. As in Figure 5, the different dashes represent different turbidity sources and the different lines represent the

mathematical model and the confidence intervals. The Eq. (10), Eq. (11) and Eq. (12) are the models represented in Figure 6. *Ryellow* ( $M\Omega$ ) represents the value of resistance in  $M\Omega$  of the LDR exposed to yellow light. The value of *Ryellow* ( $M\Omega$ ) for the same turbidity value is different according to the turbidity source. For this reason, we distinguish between *Ryellow if IG* which represents the value of resistance of the LDR with *I. galbana*, *Ryellow if TC* or *Ryellow if S* depending if the turbidity source is *Tetraselmis chuii* or sediment. Turbidity of *Isochrysis galbana* (TIG), *Tetraselmis chuii* (TTC) or sediment (TS) represents the values of turbidity in each test. The correlation coefficients of the presented mathematical models are 0.988538, 0.990275 and 0.994374 respectively. The means absolute errors are 0.0881562, 0.0642621 and 0.0586251 NTU. According to the confidence intervals, see the Figure 6, it is possible to affirm that our prototype is capable to distinguish between phytoplanktonic turbidity and sedimentary turbidity from 21.75 NTU. However, it is not able to distinguish between *Tetraselmis chuii* and *Isochrysis galbana*, according to the confidence intervals with the yellow light.

$$R_{yellow\ if\ IG}(M\Omega) = e^{(0.432322 + 0.02879 \times TIG\ (NTU))} \quad (10)$$

$$R_{yellow\ if\ TC}(M\Omega) = e^{(0.496358 + 0.0291769 \times TTC\ (NTU))} \quad (11)$$

$$R_{yellow\ if\ TS}(M\Omega) = e^{(0.606395 + 0.0105505 \times TS\ (NTU))} \quad (12)$$

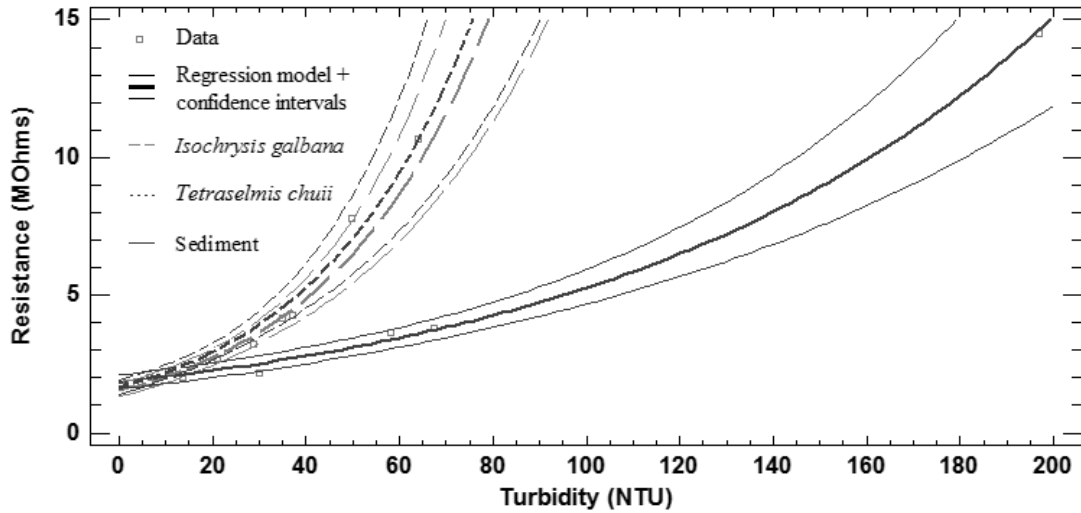


Figure 6. Regression models with confidence intervals for different turbidity sources with yellow light.

Finally, Figure 7 shows the results obtained with red light. It presents the different regression models with their confidence intervals for each one of the turbidity sources. The different dashes represent different turbidity sources. The different lines represent the mathematical model and the confidence intervals such as in Figure 5 and 6. In Figure 7 the regressions models presented correspond to the Eq. (13), Eq. (14) and Eq. (15). *Rred* ( $M\Omega$ ) is the value of resistance in  $M\Omega$  of the LDR exposed to red light. The value of *Rred* ( $M\Omega$ ) for the same turbidity value is different according to the turbidity source. For this reason, we distinguish between *Rred if IG* which represents the value of resistance of the LDR with *I. galbana*, *Rred if TC* or *Rred if S* depending if the turbidity source is *Tetraselmis chuii* or sediment. The turbidity of *Isochrysis galbana* (TIG), *Tetraselmis chuii* (TTC) or sediment (TS) represents the values of turbidity in each test. The correlation coefficients of presented regression models are 0.998397, 0.999857 and 0.989708 respectively- The means absolute errors are 0.0438597, 0.0136623 and 0.125593 NTU for each one. In this case, it is possible to affirm that our device is able to distinguish between *Tetraselmis chuii* and other turbidity sources from 12 NTU, according to the confidence intervals. Moreover, it is possible to distinguish between *Isochrysis galbana* and sediment from 16 NTU with the red light. Therefore our prototype is capable to differentiate all the tested turbidity sources by using the red light source. For this reason after

using the IR light to determine the NTU of the water, the light that will be used to identify the turbidity source is the red light.

$$R_{red\ if\ IG} (M\Omega) = e^{(0.711176 + 0.0445014 \times TIG (NTU))} \quad (13)$$

$$R_{red\ if\ TC} (M\Omega) = e^{(0.742255 + 0.0488297 \times TTC (NTU))} \quad (14)$$

$$R_{red\ if\ S} (M\Omega) = e^{(0.901301 + 0.0145908 \times TS(NTU))} \quad (15)$$

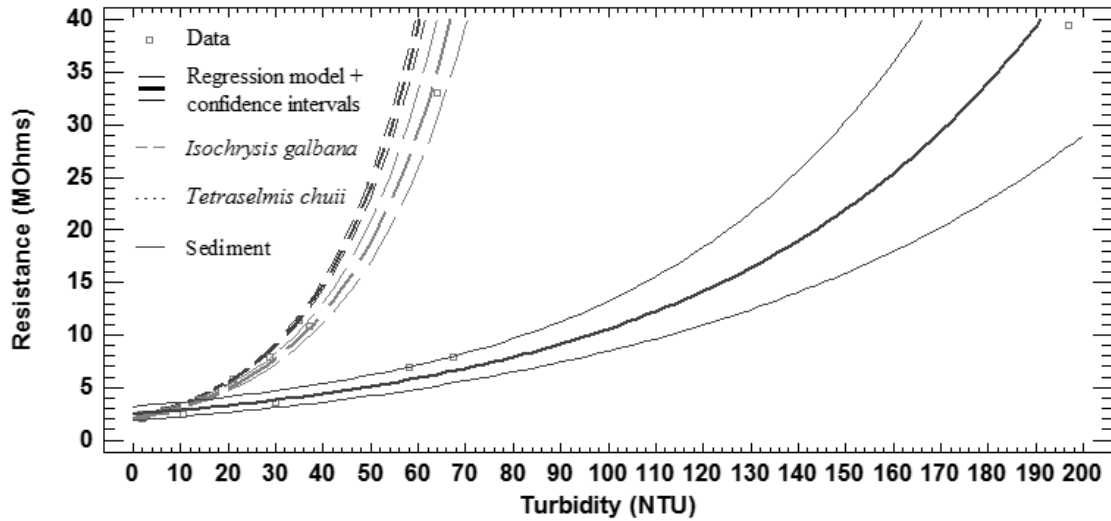
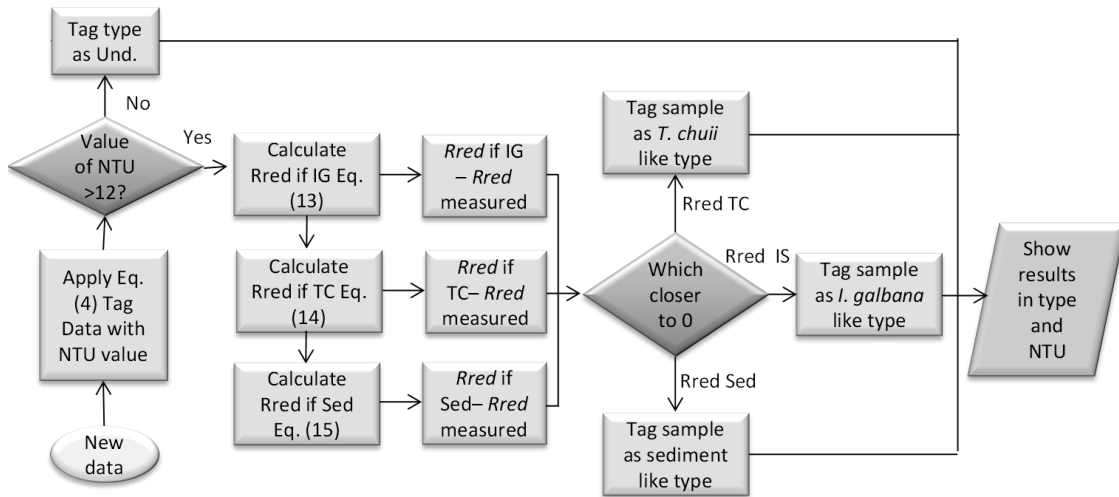


Figure 7. Regression models with confidence intervals for different turbidity sources with red light.

After analyzing all the gathered data and evaluate the confidence intervals of each mathematical model, we can conclude that the best result is obtained with the red light. It is the only light that allows distinguishing between different phytoplankton species. Besides, the red light offers the possibility to distinguish turbidity sources from the level of turbidity of 12 NTU while the other lights only can distinguish at higher turbidities, 16 and 21.75 NTU with yellow and green light. For this reason with the IR and red light, we are able to quantify the turbidity and characterize the turbidity source.

### C. Intelligent algorithm

In this subsection the algorithm used to evaluate the samples is presented, it can be seen in Algorithm 1. After a measure is done the value of resistance of IR photodiode and the value or resistance of LDR with the red light are analyzed. First, the value of resistance of IR photodiode is used in conjunction with the Eq. (4) to obtain the value of turbidity of the sample. Then, the data is tagged with the NTU value. If the NTU value is lower than 12 NTU, the data is tagged as type Undetectable (Und.). However, if the value of NTU is higher than 12 NTU the Eq. (13), Eq. (14) and Eq. (15) are applied. These equations will calculate the value expected  $R_{red}$  for a different type of turbidity sources. The model that offers a  $R_{red}$  closer to the gathered data assigns the turbidity type. Finally, the sample is tagged with the type of turbidity and with the NTU values and is shown as the result.



Algorithm 1: Decision algorithm

#### D. Verification process

In this verification process, we want to confirm that the mathematical model of our system is able to tag correctly the samples and calculate its turbidity. For this test samples were created randomly using the pure samples of algae and sediment. The samples were created by one part of the researchers and they were analyzed by researchers that do not participate in the creation of the samples. The samples were labeled as 1, 2, 3 and 4 and no information about its origin or dilution was added.

The values of resistance with IR and red light, *Rred*, were obtained using the prototype. The values of resistance with yellow and green light were not obtained because we are testing the mathematical model with the red light. First, the values of the resistance with IR light were used to calculate the turbidity of the samples. Two of the samples have turbidity values lower than 10 NTU, so according to our model, it is not possible to assign exactly the type of turbidity. The algorithm can tag the samples anyway, but it will indicate that the veracity of this label cannot be ensured.

For the next step, with the NTU values, the system calculates the expected (*Rred if IG*, *Rred if TC* and *Rred if S* (Eq13 to 15)). Finally, the measured *Rred* is compared with the expected resistance. The source of turbidity is determined by the likeness between the *Rred* and the expected resistance for each type. The results of this process can be seen in Figure 8. Figure 8 shows the *Rred* and the expected resistances calculated for the turbidity level. The first sample is tag as *I. galbana*, the second sample as sediment, the third as *T. chuii* and the last as sediment. Form the four samples, only one is tagged incorrectly and it was one of the samples with the lowest turbidity.

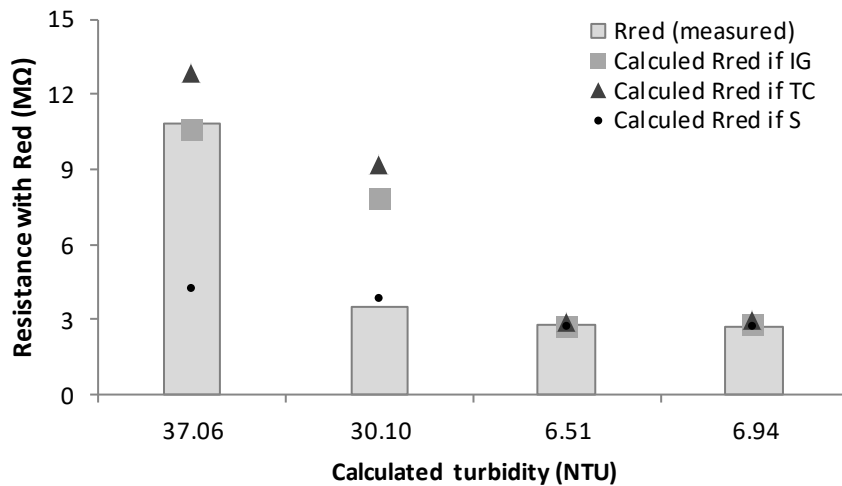


Figure 7. Regression models with confidence intervals for different turbidity sources with red light.

#### E. Comparison with current sensor systems and suitability for fish farms

In this subsection, a comparison between our developed system and the current options are performed. Moreover, we will justify the suitability of this system for fish farms.

The main advantage of the developed device and the algorithm is the capability for characterizing the turbidity. Several authors used different option based on light emission and detection to determine the water turbidity. Sendra et al., (2013a) proposed a low cost turbidity sensor, which is based on an infrared optical sensor placed at 180° of the light source. Their sensor was able to determine the turbidity of water samples, from 0 to 1000 NTU, without differentiating between turbidity sources. Shenoy et al., (2012) developed a turbidity sensor based on optical effects. Two sensors were placed at 360° from the source and a concave mirror was employed at 180° of the light source. The optic fiber was used as a light source and as a sensing element. However, their proposal is not prepared to differentiate between different turbidity sources. J. Rocher et al. (2017) presented the use of a turbidity sensor for fish farms. The sensor was based on an IR emitter and receiver. However, their turbidity sensor was not able to distinguish between different types of sediments. Goddijn-Murphy et al., (2009) analyzed of RGB values obtained with a digital camera. They affirm that there is a significant relationship in the reflectance of red and blue light for yellow substances and blue and green light for chlorophyll. However, they need the use of a digital camera and a posterior image analyzing techniques. Their development is not able to obtain data about the IR region. Moreover, they do not make a relation between the color and the concentration of the substances.

Different authors proposed the application of remote sensing to quantify the turbidity. Tyler et al., (2006) were able to determine the concentration of suspended solids and chlorophyll in lakes. Sebastia et al., (2012) demonstrated the capability of using remote sensing to determine the concentration of chlorophyll *a* in coastal areas of the Mediterranean sea. However, the use of remote sensing it is not useful for continuous monitoring due to the low temporal resolution of the images. Moreover, it is not useful for monitoring the changes inside the aquaculture facilities. It can be useful to monitor the changes in the water body from which the water is obtained.

Chanson et al., (2008) proposed to use an Acoustic Doppler Velocimeter (ADV) with backscattering to determine the turbidity in water bodies. Event that this methodology offered good correlation, it is not possible to characterize the origin of the turbidity. Vousdoukas et al., (2011) proposed a similar system. The proposed prototype in this paper is able to differentiate different types of turbidity. Moreover, the use of ADV in fish farms facilities is not a suitable option because of the small volume of water and the continuous changes of velocity along the facilities.

As a summary, the systems based on remote sensing are not suitable for inland fish farms facilities that can be covered or placed inside the building. Besides, the temporal resolution is not enough to ensure a continuous monitoring. The systems based on ADV are able to distinguish turbidity types, but it is not indicated for small water volumes. Then, the most indicated system is the one based on light absorption. The current systems based on light absorption are appropriated for water quality monitoring in fish farms. Nevertheless, they are not able to distinguish between turbidity sources. The developed sensor in this paper shows how using two light sources with different wavelength and two detectors it is possible to distinguish different turbidity sources. This system can monitor the turbidity giving, as a result, the water turbidity in NTU and the type of turbidity: sediment, green phytoplankton or brown phytoplankton. For fish farming the capacity to distinguish between types of turbidity is important.

#### IV. CONCLUSIONS

In this paper, we design, develop and calibrate a turbidity sensor for water, which is able to determine the turbidity and to differentiate between sedimentary and phytoplanktonic turbidity. The prototype is based on the Beer-Lambert law and the absorption of light by the turbidity. The sensor uses four different light sources with different wavelengths: IR, green, yellow and red. Two different light receptors placed at 180° of light sources were employed, IR photodiode and LDR sensible to the visible spectrum. The calibration was performed with two species of phytoplankton and with sediment. The results show that the prototype is able to distinguish between different algae species and sediment using the value of LDR with the red light as a source. An algorithm was developed to endow our prototype with the ability to differentiate between turbidity sources based on the resistance of the LDR and photodiode. The algorithm is based on the empiric equations obtained in the calibration process. Our findings allow to obtain turbidity measures in fish farms facilities and to characterize this turbidity in order to take the necessary actions to prevent further damages.

Our future work is focused on creating a wireless sensor network (WSN) composed by this turbidity sensor and other sensors for water quality monitoring similar to the proposed system by Sendra et al., (2015). Moreover, we pretend to deploy this WSN in a fish farm facility to control the water parameters along the facility. We will prepare a new set of samples mixing sediment and phytoplankton in order to find out if the sensor can distinguish the percentage of each turbidity source in case of turbidity caused by two sources. Moreover, we want to include our prototype in an alarm system similar to the one developed by J. Rocher-Morant (2017) but including different types of alarms according to the turbidity source.,

#### ACKNOWLEDGMENT

This work has been partially supported by the “Ministerio de Educación, Cultura y Deporte”, through the “Ayudas para contratos predoctorales de Formación del Profesorado Universitario FPU (Convocatoria 2014)”. Grant number FPU14/02953.

#### REFERENCES

- APHA, AWWA, WEF. Standard Methods for examination of water and wastewater. 22nd ed. Washington: American Public Health Association; 2012, 1360 pp. ISBN 978-087553-013-0
- Ardjosoediro, I., & Ramnarine, I. W. 2002. The influence of turbidity on growth, feed conversion and survivorship of the Jamaica red tilapia strain. *Aquaculture*, 212(1), 159-165.
- Au, D. W. T., Pollino, C. A., Wu, R. S. S., Shin, P. K. S., Lau, S. T. F., & Tang, J. Y. M. 2004. Chronic effects of suspended solids on gill structure, osmoregulation, growth, and triiodothyronine in juvenile green grouper *Epinephelus coioides*. *Marine ecology progress series*, 266, 255-264.
- Beaudeau, P., Schwartz, J., & Levin, R. 2014. Drinking water quality and hospital admissions of elderly people for gastrointestinal illness in Eastern Massachusetts, 1998–2008. *Water research*, 52, 188-198

- Bin Omar, A. F., & Bin MatJafri, M. Z. 2009. Turbidimeter design and analysis: a review on optical fiber sensors for the measurement of water turbidity. *Sensors*, 9(10), 8311-8335.
- Bruton, M. N. 1985. The effects of suspensoids on fish. *Hydrobiologia*, 125(1), 221-241.
- Chanson, H., Takeuchi, M., & Trevethan, M. 2008. Using turbidity and acoustic backscatter intensity as surrogate measures of suspended sediment concentration in a small subtropical estuary. *Journal of environmental management*, 88(4), 1406-1416.
- Eureqa, 2017. <https://www.nutonian.com/products/eureqa/> (Last Access: November 22, 2017)
- Fabricius, K. E., Logan, M., Weeks, S. J., Lewis, S. E., & Brodie, J. 2016. Changes in water clarity in response to river discharges on the Great Barrier Reef continental shelf: 2002–2013. *Estuarine, Coastal and Shelf Science*, 173, A1-A15.
- Faulk, C. K., & Holt, G. J. 2005. Advances in rearing cobia *Rachycentron canadum* larvae in recirculating aquaculture systems: live prey enrichment and greenwater culture. *Aquaculture*, 249(1), 231-243.
- Goddijn-Murphy, L., Dailoux, D., White, M., & Bowers, D. 2009. Fundamentals of in situ digital camera methodology for water quality monitoring of coast and ocean. *Sensors*, 9(7), 5825-5843.
- Güttler, F. N., Niculescu, S., & Gohin, F. 2013. Turbidity retrieval and monitoring of Danube Delta waters using multi-sensor optical remote sensing data: An integrated view from the delta plain lakes to the western–northwestern Black Sea coastal zone. *Remote Sensing of Environment*, 132, 86-101.
- Hess, S., Wenger, A. S., Ainsworth, T. D., & Rummer, J. L. 2015. Exposure of clownfish larvae to suspended sediment levels found on the Great Barrier Reef: Impacts on gill structure and microbiome. *Scientific reports*, 5, 10561.
- Keller, M.D., Selvin, R.C., Claus, W., & Guillard, R.R.L., 1987. Media for the culture of oceanic ultraphytoplankton. *Journal of Phycology*, 23, 633-638.
- Lambrou, T. P., Anastasiou, C. C., & Panayiotou, C. G. (2009). A nephelometric turbidity system for monitoring residential drinking water quality. In *Proceedings of the Sensor Applications, Experimentation and Logistics*, Athens, Greece, September 25, 2009, 43-55.
- LDR, 2017. <http://lunainc.com/wp-content/uploads/2016/06/NSL-19M51.pdf> (Last access: November 22, 2017)
- Lee, J. S. 2015. Clay As a Greenwater Alternative for Larval Sablefish *Anoplopoma fimbria*. In *Proceedings of the 145th Annual Meeting of the American Fisheries Society*, Portland, Oregon, 16 – 20 August, 2015.
- Lee, J. S., Cook, M. A., Berejikian, B. A., & Goetz, F. W. 2017. Temporal changes in the suitability of claywater as a greenwater substitute for rearing larval sablefish (*Anoplopoma fimbria*). *Aquaculture*, 470, 11-16.
- Lee, Z., Shang, S., Hu, C., Du, K., Weidemann, A., Hou, W., Lin, J. & Lin, G. 2015. Secchi disk depth: A new theory and mechanistic model for underwater visibility. *Remote Sensing of Environment*, 169, 139-149.
- MPCA (Minnesota Pollution control Agency), Turbidity: Description, Impact on Water Quality, Sources, Measures Available at : <https://www.pca.state.mn.us/sites/default/files/wq-iw3-21.pdf> (Last access: february 21, 2017).

- Palmer, P. J., Burke, M. J., Palmer, C. J., & Burke, J. B. 2007. Developments in controlled green-water larval culture technologies for estuarine fishes in Queensland, Australia and elsewhere. *Aquaculture*, 272(1), 1-21.
- Parra, L., Sendra, S., Lloret, J., & Rodrigues, J. J. 2014. Low cost wireless sensor network for salinity monitoring in mangrove forests. In *Proceedings of the IEEE SENSORS 2014*, Valencia, Spain, 02 - 05 Nov 2014 (pp. 126-129).
- Parra, L., Sendra, S., Jimenez, J. M., & Lloret, J. 2015. Smart system to detect and track pollution in marine environments. In *Proceedings of the 2015 IEEE International Conference on Communication Workshop*, London, U.K., 8 – 12 Jun 2015 (pp. 1503-1508).
- Parra, L., Sendra, S., Lloret, J., & Rodrigues, J. J. 2017. Design and deployment of a smart system for data gathering in aquaculture tanks using wireless sensor networks. *International Journal of Communication Systems*.
- PNUMA, Metodología para el establecimiento de niveles guía de calidad de agua ambiente para riego Available at : <http://www.pnuma.org/agua-miaac/CODIA%20CALIDAD%20DE%20LAS%20AGUAS/MATERIAL%20ADICIONAL/PONENCIAS/PONENTES/Tema%205%20Niveles%20Guias%20Calidad%20de%20Aguas/NIVELES%20GUIA/2%20-%20Metodologias/3%20-%20Metodologia%20Riego.pdf> (Last access: January 12, 2017).
- Postolache, O., Girao, P., Pereira, M., & Ramos, H. 2002. An IR turbidity sensor: design and application. In *Proceedings of the 19th IEEE Instrumentation and Measurement Technology Conference IMTC/2002*, Alaska, USA, 21-23 May, 2002, 535-539.
- Rocher, J., Taha, M., Parra, L., & Lloret, J. 2007. Design and deployment of a WSN for water turbidity monitoring in fish farms. In *Proceedings of the 10th IFIP Wireless and Mobile Networking Conference (WMNC)*, 2017, Valencia, Spain, 25-27 sept 2017,
- Schoellhamer, D. H., & Wright, S. A. 2003. Continuous measurement of suspended-sediment discharge in rivers by use of optical backscatterance sensors. *IAHS PUBLICATION*, 28-36
- Sebastiá, M. T., Estornell, J., Rodilla, M., Martí, J., & Falco, S. 2012. Estimation of chlorophyll «A» on the Mediterranean coast using a QuickBird image. *Revista de Teledetección*, 37, 23-33.
- Sendra, S., Parra, L., Ortuno, V., & Lloret, J. 2013a. A low cost turbidity sensor development. In *Proceedings of the 7th International Conference on Sensor Technologies and Applications SENSORCOMM'13*, Barcelona, Spain, 25 – 31 August, 2013, 266-272
- Sendra, S., Llarío, F., Parra, L., & Lloret, J. 2013b. Smart wireless sensor network to detect and protect sheep and goats to wolf attacks. *Recent Advances in Communications and Networking Technology (Formerly Recent Patents on Telecommunication)*, 2(2), 91-101.
- Sendra, S., Parra, L., Lloret, J., & Jiménez, J. M. 2015. Oceanographic multisensor buoy based on low cost sensors for posidonia meadows monitoring in Mediterranean Sea. *Journal of Sensors*, 2015.
- Shenoy, M. R., Pal, B. P., & Gupta, B. D. (2012). Design, analysis, and realization of a turbidity sensor based on collection of scattered light by a fiber-optic probe. *IEEE Sensors Journal*, 12(1), 44-50.
- Smith, D., & Davis-Colley, R. (2001). Turbidity suspended sediment and water clarity. *J Am Water Resour Assoc*, 37, 1085-1101.

- STATGRAPHICS, 2017. <http://www.statgraphics.net/descargas-centurion-xvii/> (Last access: February 24, 2017)
- Stubblefield, A. P., Reuter, J. E., Dahlgren, R. A., & Goldman, C. R. (2007). Use of turbidometry to characterize suspended sediment and phosphorus fluxes in the Lake Tahoe basin, California, USA. *Hydrological Processes*, 21(3), 281-291.
- Sutherland, A. B., & Meyer, J. L. (2007). Effects of increased suspended sediment on growth rate and gill condition of two southern Appalachian minnows. *Environmental Biology of Fishes*, 80(4), 389-403.
- Takaaki, A. B. E., Mizugaki, S., Toyabe, T., Maruyama, M., Murakami, Y., & Ishiya, T. (2012). High range turbidity monitoring in the Mu and Saru river basins: All-year monitoring of hydrology and suspended sediment transport in 2010. *International Journal of Erosion Control Engineering*, 5(1), 70-79.
- Tyler, A. N., Svab, E., Preston, T., Présing, M., & Kovács, W. A. 2006. Remote sensing of the water quality of shallow lakes: A mixture modelling approach to quantifying phytoplankton in water characterized by high-suspended sediment. *International Journal of Remote Sensing*, 27(8), 1521-1537.
- LDR, 2017. [http://www.farnell.com/datasheets/77395.pdf?\\_ga=2.27766780.1568076438.1510680363-1814763420.1510680363](http://www.farnell.com/datasheets/77395.pdf?_ga=2.27766780.1568076438.1510680363-1814763420.1510680363) (Last access: November 14, 2017)
- Vishay, 2017a. <https://www.vishay.com/docs/81078/tshg6200.pdf> (Last access: November, 2017)
- Vishay, 2017b. <http://www.vishay.com/docs/83029/tllg440.pdf> (Last access: February 24, 2017)
- Vishay, 2017c. <http://www.vishay.com/docs/81530/bpw83.pdf> (Last access: February 24, 2017)
- Vousdoukas, M. I., Aleksiadis, S., Grenz, C., & Verney, R. (2011). Comparisons of acoustic and optical sensors for suspended sediment concentration measurements under non-homogeneous solutions. *Journal of coastal research*, 64, 160-164.
- Ward, D. P., Hamilton, S. K., Jardine, T. D., Pettit, N. E., Tews, E. K., Olley, J. M., & Bunn, S. E. 2013. Assessing the seasonal dynamics of inundation, turbidity, and aquatic vegetation in the Australian wet-dry tropics using optical remote sensing. *Ecohydrology*, 6(2), 312-323.
- Wilber, D. H., & Clarke, D. G. 2001. Biological effects of suspended sediments: a review of suspended sediment impacts on fish and shellfish with relation to dredging activities in estuaries. *North American Journal of Fisheries Management*, 21(4), 855-875.
- Zheng, Z., Ren, J., Li, Y., Huang, C., Liu, G., Du, C., & Lyu, H. 2016. Remote sensing of diffuse attenuation coefficient patterns from Landsat 8 OLI imagery of turbid inland waters: A case study of Dongting Lake. *Science of The Total Environment*, 573, 39-54.